J Pharmacokinet Pharmacodyn (2011) 38:713–725
DOI 10.1007/s10928-011-9216-2

Mechanism-based population modelling for assessment of L-cell function based on total GLP-1 response following an oral glucose tolerance test

Jonas B. Møller · William J. Jusko · Wei Gao · Torben Hansen · Oluf Pedersen · Jens J. Holst · Rune V. Overgaard · Henrik Madsen · Steen H. Ingwersen

Received: 13 December 2010 / Accepted: 8 September 2011 / Published online: 16 September 2011
© Springer Science+Business Media, LLC 2011

Abstract GLP-1 is an insulinotropic hormone that synergistically with glucose gives rise to an increased insulin response. Its secretion is increased following a meal and it is thus of interest to describe the secretion of this hormone following an oral glucose tolerance test (OGTT). The aim of this study was to build a mechanism-based population model that describes the time course of total GLP-1 and provides indices for capability of secretion in each subject. The goal was thus to model the secretion of GLP-1, and not its effect on insulin production. Single 75 g doses of glucose were administered orally to a mixed group of subjects ranging from healthy volunteers to patients with type 2 diabetes (T2D). Glucose, insulin, and total GLP-1 concentrations were measured. Prior population data analysis on measurements of glucose and insulin were performed in order to estimate the glucose absorption rate. The individual estimates of absorption rate constants were used in the model for GLP-1 secretion. Estimation of parameters was performed using the FOCE method with interaction implemented in NONMEM VI. The final transit/

J. B. Møller (✉) · R. V. Overgaard · S. H. Ingwersen
Quantitative Clinical Pharmacology, Novo Nordisk A/S, Søborg, Denmark
e-mail: jbem@novonordisk.com

W. J. Jusko · W. Gao
Department of Pharmaceutical Sciences, State University of New York at Buffalo, Buffalo, NY, USA

T. Hansen · O. Pedersen
Hagedorn Research Institute, Gentofte, Denmark

J. J. Holst
Department of Medical Physiology, Panum Institute, University of Copenhagen, Copenhagen, Denmark

H. Madsen
Department of Informatics and Mathematical Modelling, Technical University of Denmark, Lyngby, Denmark

Apotex v. Novo - IPR2024-00631
Petitioner Apotex Exhibit 1053-0001

MPI EXHIBIT 1053 PAGE 1

indirect-response model obtained for GLP-1 production following an OGTT included two stimulation components (fast, slow) for the zero-order production rate. The fast stimulation was estimated to be faster than the glucose absorption rate, supporting the presence of a proximal–distal loop for fast secretion from L-cells. The fast component ($st_3 = 8.64 \cdot 10^{-5}$ [mg^{-1}]) was estimated to peak around 25 min after glucose ingestion, whereas the slower component ($st_4 = 26.2 \cdot 10^{-5}$ [mg^{-1}]) was estimated to peak around 100 min. Elimination of total GLP-1 was characterised by a first-order loss. The individual values of the early phase GLP-1 secretion parameter (st_3) were correlated ($r = 0.52$) with the AUC(0–60 min.) for GLP-1. A mechanistic population model was successfully developed to describe total GLP-1 concentrations over time observed after an OGTT. The model provides indices related to different mechanisms of subject abilities to secrete GLP-1. The model provides a good basis to study influence of different demographic factors on these components, presented mainly by indices of the fast- and slow phases of GLP-1 response.

Keywords GLP-1 · L-cells · Oral glucose tolerance test (OGTT) · Indirect response model · NONMEM

Introduction

Type 2 diabetes (T2D) is a result of decreased insulin sensitivity combined with decreased beta-cell function. The beta-cell function is described by the ability of the beta-cells to provide an insulin response to a given glucose load.

One of the main determinants of beta-cell function is the presence of the insulinotropic hormone glucagon-like-peptide 1 (GLP-1) [1, 2] in combination with glucose. More specifically Brandt et al. [2] demonstrated in vivo glucose dependency of the action of postprandial physiological concentrations of GLP-1 in healthy subjects over the plasma glucose range of 5–10 mM.

GLP-1 is a gut derived peptide secreted from intestinal L-cells [3] and circulating levels increase after a meal or an oral glucose load [4, 5]. It is derived from a transcription product of the proglucagon gene and the active molecule is identified as GLP-1 (7–36). Once in the circulation it has a very short half-life estimated to be around 2–3 min in healthy volunteers [4].

The GLP-1 response in terms of area under the curve from 0 to 240 min. after the start of the meal is significantly decreased in most patients with type 2 diabetes [6]. Combined with the finding that the short half-life of GLP-1 does not seem to differ in healthy volunteers and patients with T2D [1], this suggests that the decreased GLP-1 response observed in patients with T2 diabetes is due to a lower post-prandial secretion. This also seems to be the case comparing patients with impaired glucose tolerance (IGT) and healthy volunteers [5]. In general we believe that analysis of the GLP-1 response observed after an OGTT would be valuable in understanding the mechanisms underlying the post-prandial secretion profile.

The overall aim of this study was to develop a mechanism-based population model providing descriptive indices of the observed GLP-1 secretion following an

Apotex v. Novo - IPR2024-00631
Petitioner Apotex Exhibit 1053-0002
MPI EXHIBIT 1053 PAGE 2

OGTT. The goal was thus not to model the GLP-1 effect on insulin secretion, but rather to build a model providing indices for capability of GLP-1 secretion. Based on the mechanisms of action, we propose to model the stimulation of GLP-1, using an indirect response model [7]. Compared to earlier non-compartmental analysis (as in [8]) of the GLP-1 secretion profiles observed after an OGTT, a compartmental population model approach takes into account variability in measurements and time (compartmental) and variability between subjects (population). This kind of model further provides a good basis for future inclusion of covariates (such as demographic factors) on obtained model parameters.

Methods

Study participants

The data applied in this study is a subset of the dataset originally described in [9]. In this study available plasma GLP-1 profiles obtained after an oral glucose load are included. Only full profiles were included and seven profiles were removed because of erratic behaviour inconsistent with basic physiology and the dynamics of the rest of the population. The cleaned dataset applied here thus consisted of samples taken from 135 individuals distributed as presented in Table 1. The classification of individuals was categorized according to concentrations of plasma glucose (FPG) fasting and 2 h after glucose ingestion ($OGTT_{120}$) measured in mmol/L. The classification criteria, agreed with the ones described in [10]. The study was approved by the Ethical Committee of Copenhagen and was in accordance with the principles of the Declaration of Helsinki.

Study conditions

All participants underwent a standardized and extended 75-g frequently sampled OGTT. After a 12-h overnight fast, venous blood samples were drawn in duplicate at −30, −10, 0 before the glucose intake and then at 10, 20, 30, 40, 50, 60, 75, 90, 105, 120, 140, 160, 180, 210, 240. Plasma glucose and serum insulin were measured. The plasma glucose concentration was analyzed by a glucose oxidase method (Granutest; Merck, Darmstadt, Germany). Serum insulin was determined by

Table 1 Mean and standard deviation (SD) of demographics of study subjects

Subjects	Normal	IFG-IGT-T2D	Total
Number	117	18	135
Age [yr]	41.8 (11.4)	45.6 (12.7)	42.3 (11.6)
Fasting plasma glucose [mg dl^{-1}]	93.0 (8.1)	109.8 (13)	95.3 (10.5)
Fasting plasma insulin [pmol l^{-1}]	5.43 (3.1)	11.66 (8.4)	6.26 (4.6)
Fasting plasma GLP-1(total) [pmol l^{-1}]	5.35 (3.3)	4.61 (2.6)	5.26 (3.2)

IFG Impaired fasting glucose, *IGT* Impaired glucose tolerance, *T2D* Type 2 diabetics

Apotex v. Novo - IPR2024-00631
Petitioner Apotex Exhibit 1053-0003

MPI EXHIBIT 1053 PAGE 3

enzyme-linked immunoadsorbent assay with a narrow specificity excluding des (31, 32)-proinsulin and intact proinsulin (DAKO Diagnostics, Ely, UK) [11].

Fasting plasma GLP-1 were analysed in duplicate and at single measurements post glucose load at time points 10, 20, 30, 40, 60, 90, 120, 180, and 240 min. All blood samples for GLP-1 analysis were kept on ice, and the protease inhibitor aprotinin (Novo Nordisk, Denmark) was added in a concentration of 0.08 mg/ml blood. The GLP-1 concentrations were measured after extraction of plasma with 70% ethanol (vol/vol). The plasma concentrations of GLP-1 were measured [12] using standards of synthetic GLP-1 7–36 amide using antiserum code no. 89390, which is specific for the amidated C-terminus of GLP-1 and therefore mainly reacts with GLP-1 derived from the intestine. The results of the assay reflect the rate of secretion of GLP-1 because the assay measures the sum of intact GLP-1 and the primary metabolite, GLP-1 9–36 amide, into which GLP-1 is rapidly converted [13]. The assay sensitivity was below 1 pmol/l, intra-assay coefficient of variation below 0.06 at 20 pmol/l, and recovery of standard added to plasma before extraction was 100% when corrected for losses inherent in the plasma extraction procedure. Very few samples were under the LLOQ, and these were not included in analysis.

Non-compartmental analysis

The individual incremental areas under the curve for GLP-1 were calculated using a linear up/linear down trapezoidal method. Peak AUCs identified in the report as $AUCP_{GLP\text{-}1}$ were calculated as incremental AUCs up to 60 min. The software S-plus was used for this part of the analysis.

Compartmental population modelling

For preliminary analysis, the absorption rate constant (k_a) of glucose was obtained from glucose and insulin data by applying the model presented by Lima et al. [14], using two compartments for description of absorption rate according to Eq. (3) and (4). This was done in order not to bias the estimation of this parameter towards the fitting of GLP-1.

Baseline GLP-1 values were calculated as the average from pre-dose samples for each individual. Considering the fact that the inclusion of these baseline values as either fixed or estimated can influence the bias of other parameters [15], we implemented these values as either fixed, fixed with a variance, or estimated. In general the GLP-1 data was modelled using a population model build in NONMEM VI using the FOCE Inter method. Model selection was based on individual/population predicted profiles, variance and independence of residuals, and obtained objective function value (OFV), and inspection of visual predictive check (VPC).

Structural model

The final structural models for glucose/insulin and secretion of GLP-1 are presented in Fig. 1. The glucose/insulin model was applied in order to obtain estimates of glucose absorption rate. The model for the GLP-1 secretion reflects an indirect

Apotex v. Novo - IPR2024-00631
Petitioner Apotex Exhibit 1053-0004
MPI EXHIBIT 1053 PAGE 4

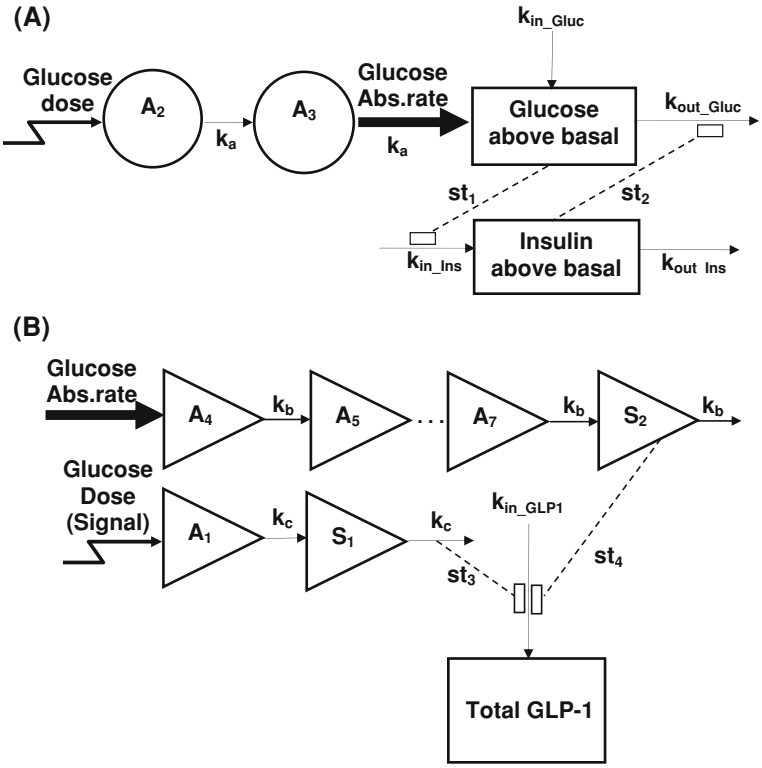


Fig. 1 **a** Diagram of glucose/insulin model for estimation of glucose absorption rate constant, **b** GLP-1 secretion model. Absorption rate for glucose is identical to that estimated in the glucose/insulin model. Symbols are defined in Table 2

response model with zero-order input and first-order loss. The zero-order input was found to be stimulated by two mechanisms differentiated by time of onset. The first part was estimated to be faster than the absorption of glucose and caused a peak in the GLP-1 concentration around 40 min as also identified in [16]. The ingestion signal was included as being proportional to the glucose dose size as:

$$\frac{dA_1}{dt} = -k_c \cdot A_1, \quad A_1(0) = Dose \tag{1}$$

$$\frac{dS_1}{dt} = k_c \cdot A_1 - k_c \cdot S_1, \quad S_1(0) = 0 \tag{2}$$

where $1/k_c$ [min] determines the length of the signal caused by the intake of the amount of glucose, defined by *D*ose. The A_1 and S_1 define the first and second transit compartments in the early response signal originating from ingestion of glucose. The second part was related to a delayed version of the absorption of glucose in gut. The delay was implemented with the use of transit compartments.

The optimal number of transit compartments for description of the delay was determined based on an explicit solution [17] together with the obtained OF Vs.

Apotex v. Novo - IPR2024-00631
Petitioner Apotex Exhibit 1053-0005

MPI EXHIBIT 1053 PAGE 5

From the obtained number of compartments and rate constants, this signal was identified to peak around 100 min. The equations below define the glucose absorption rate ($k_a \cdot A_3$) and the stimulus of GLP-1 production related to the absorption rate (S_2).

$$\frac{dA_2}{dt} = -k_a \cdot A_2, \quad A_2(0) = Dose \cdot f \tag{3}$$

$$\frac{dA_3}{dt} = k_a \cdot A_2 - k_a \cdot A_3, \quad A_3(0) = 0 \tag{4}$$

$$\frac{dA_4}{dt} = k_a \cdot A_3 - k_b \cdot A_4, \quad A_4(0) = 0 \tag{5}$$

$$\frac{dA_5}{dt} = k_b \cdot A_4 - k_b \cdot A_5, \quad A_5(0) = 0 \tag{6}$$

$$\vdots$$

$$\frac{dS_2}{dt} = k_b \cdot A_6 - k_b \cdot S_2, \quad S_2(0) = 0 \tag{7}$$

The value of f was fixed to 0.722 based on the bioavailability of glucose observed from an OGTT in healthy subjects [18].

Specifically A_2 presents the glucose at absorption site, and $k_a \cdot A_3$ the glucose absorption rate as stated above. The absorption rate constant k_a was estimated using the compartment absorption structure of glucose (A_2 and A_3) connected to an indirect response model for the interaction between glucose and insulin [14], see Fig. 1. The rate constant k_b defines the delay between glucose absorption rate and stimulation of late-phase GLP-1 secretion. The S_2 thus defines the signal related to stimulation of GLP-1 production by glucose absorption.

The elimination of GLP-1 was implemented as a first-order process. In total, the concentration of total GLP-1 following the OGTT is described by

$$\begin{aligned} &\frac{dC_{GLP1}}{dt} = k_{in_GLP1} \cdot [1 + st_3 \cdot S_1 + st_4 \cdot S_2] - k_{out_GLP1} \cdot C_{GLP1}, \\ &C_{GLP1}(0) = B_{GLP1} \end{aligned} \tag{8}$$

where k_{in_GLP1} (pmol $l^{-1} \cdot min^{-1}$) is the endogenous production rate of GLP-1 and k_{out_GLP1} (min^{-1}) the first-order rate constant of GLP-1 elimination with the steady-state condition defined by

$$k_{in_GLP1} = B_{GLP1} \cdot k_{out_GLP1} \tag{9}$$

where B_{GLP1} is the baseline level of GLP-1. The parameters st_3 and st_4 present first- and second-phase stimulation factors related to the first- and second phase stimulation signals (S_1 and S_2).

Individual model

Inclusion of Inter-individual variability (IIV) was done according to a log-normal distribution of individual parameters. The IIV was included for all estimated

Apotex v. Novo - IPR2024-00631
Petitioner Apotex Exhibit 1053-0006
MPI EXHIBIT 1053 PAGE 6

parameters except k_{out_GLP1} which is experimentally found not to vary significantly between subjects [1]. Due to a high correlation, the same random effect was used for st_3 and st_4, and these were estimated according to

$$st_3 = \theta_1 \cdot \exp(\eta_1) \tag{10}$$

$$st_4 = \theta_2 \cdot \exp(\kappa \cdot \eta_1) \tag{11}$$

where θ_1 is the typical value of st_3 and η_1 the random effects parameter related to the inter-subject variability of st_3 and similar for st_4. Note that the inter-variability between the individual estimates of st_4 is proportional to the inter-variability of the st_3 estimates using the constant κ.

Residual error model

Additive, proportional, and combined error models were tested. The combined error model appeared superior.

Results

Four individual GLP-1 concentration versus time profiles together with model predictions are shown in Fig. 2. High variability in the profiles is present both for the baseline and in the dynamics of the GLP-1 hormone.

Figure 3 presents population predictions together with individual observations and their mean. Figure 4 presents the autocorrelation function (ACF) of residuals [19]. A visual predictive check (VPC) of the model is presented in Fig. 5. These figures indicate that the model seems to adequately capture the main GLP-1 dynamics measured in the studied population. There is no need to implement the presented model using stochastic differential equations (SDEs). This is augmented by the fact that for all lags >0 there is small correlation and only the correlation at lag = 2 (corresponding to the correlation between residuals shifted two time-points) is significant (See Fig. 4).

Interpretation, estimated values, and inter-individual variability (IIV) of each parameter is presented in Table 2. For each parameter estimated with IIV we have also reported the η-shrinkages (*shr*) as these measures are of importance e.g. for a study incorporating covariate effects [20]. The shrinkage on the residual error was found to be very small.

In order to check that our model was consistent with NCA-analysis, we plotted the fast stimulation index st_3 versus $AUCP_{GLP\text{-}1}$ which has been used previously [21] to measure the size of the fast response (see Fig. 6). A significant correlation between the two measures ($r = 0.52$) was obtained.

Figure 7 presents the time course of mean signals related to the fast and the slow GLP-1 responses (simulation of compartment S_1 and S_2 above using the estimated typical values of k_a, k_b and k_c) together with the mean of simulated A_3, the presenting compartment related to glucose absorption rate. For the fast response a

Apotex v. Novo - IPR2024-00631
Petitioner Apotex Exhibit 1053-0007

MPI EXHIBIT 1053 PAGE 7

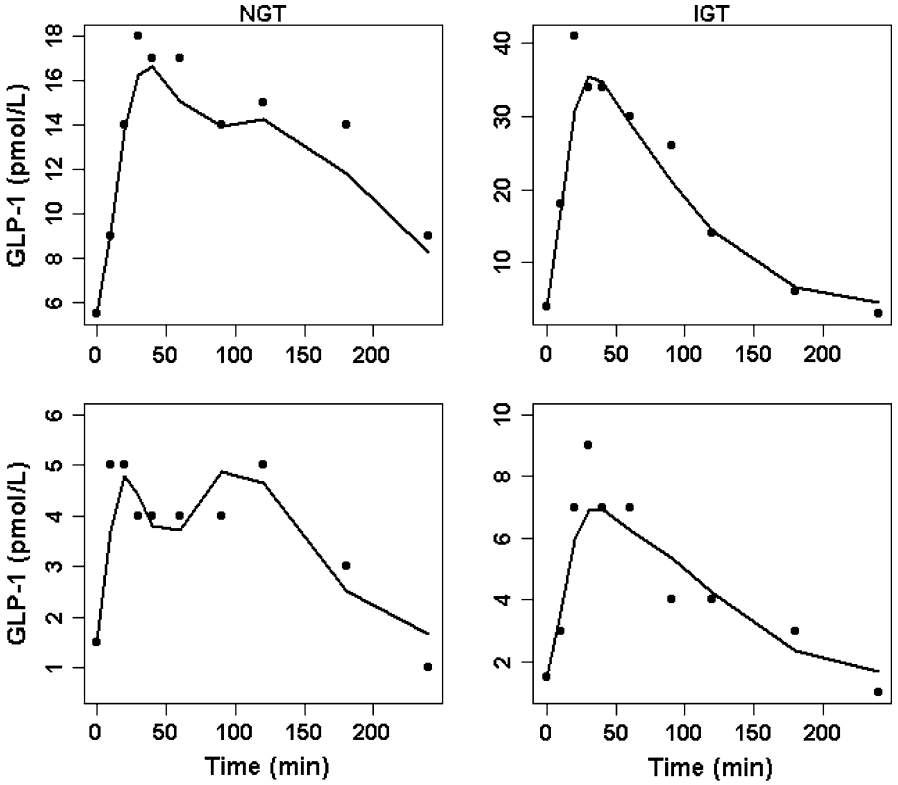


Fig. 2 Measurements and individual predictions of total GLP-1 versus time after the oral dose of glucose. *Left*: Normal glucose tolerant subjects (NGT). *Right*: Impaired glucose tolerant subjects (IGT)

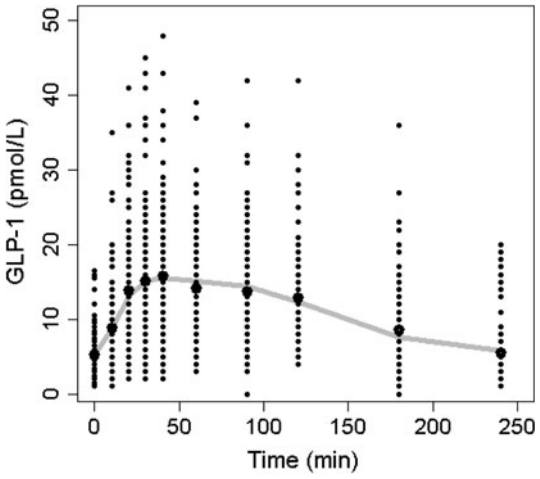


Fig. 3 Comparison between mean DV and population prediction. *Black small dots*: plasma concentrations of GLP-1 versus time for all subjects. *Large dots*: mean observed GLP-1 concentrations. *Gray curve*: population prediction

Apotex v. Novo - IPR2024-00631
Petitioner Apotex Exhibit 1053-0008
MPI EXHIBIT 1053 PAGE 8

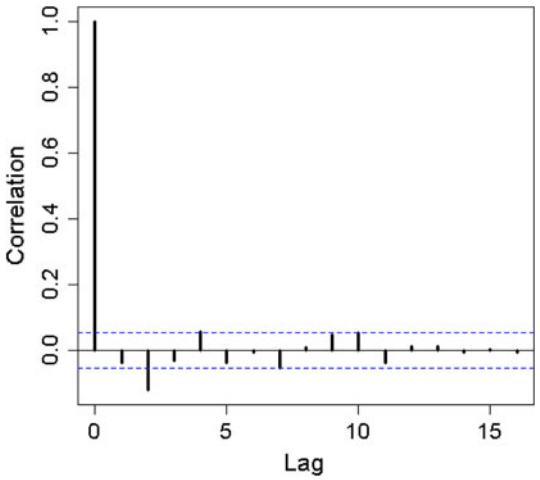


Fig. 4 Autocorrelation function (ACF) calculated based on appended residuals from each subject

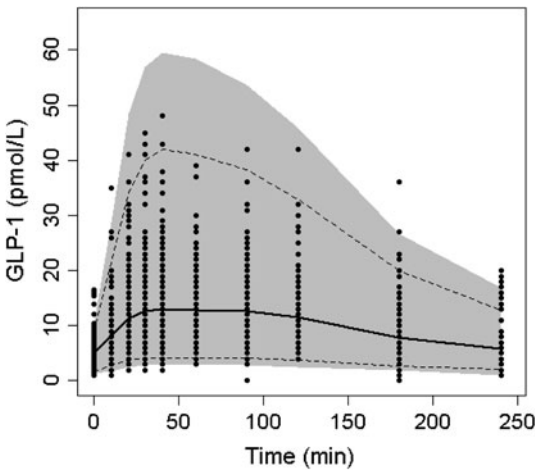


Fig. 5 Visual predictive check (VPC) of GLP-1 measurements versus time. Shaded area defines the 5–95th percentiles of predictions and *dotted line*, the 10–90th percentiles for predictions. *Full line* presents median of prediction, whereas *dots* represent data points

peak around 25 min is observed, whereas the slow response peaked around 100 min.

Discussion

In this study we modelled the sum of intact GLP-1 and the primary metabolite, GLP-1 (9–36), into which GLP-1 is rapidly converted. This sum therefore reflects the rate of secretion of GLP-1. The obtained total GLP-1 concentrations following the OGTT could be described by an indirect response model with zero-order production rate and first-order loss. Stimulation of GLP-1 production by glucose was characterized with a fast stimulation signal and a signal related to a delayed version of the absorption rate of glucose. Elimination was characterized by a non-saturable

Apotex v. Novo - IPR2024-00631
Petitioner Apotex Exhibit 1053-0009

MPI EXHIBIT 1053 PAGE 9

Table 2 Obtained parameter estimates for GLP-1 dynamics

Parameter	Interpretation	Value	SEM (%)	IIV (CV%)	Shr (%)
f (−)	*Absorption fraction*	*0.722*	–	–	–
k_a (min^{-1})	Abs. rate constant	0.0359	2	0.0581(24)	5
k_b (min^{-1})	Transit rate constant	0.0962	8	0.0357(12)	20
k_c (min^{-1})	Neural signal rate constant	0.0566	11	0.270(52)	20
k_{out_GLP1} (min^{-1})	First-order elimination rate constant of GLP-1	0.0644	18	0 FIXED	–
κ [−]	Proportionality between IIV on st_3 and st_4	0.775	10	0 FIXED	–
st_3 [mg^{-1}]	Stimulation factor of GLP-1 production by early signal	$8.64 \cdot 10^{-5}$	10	0.939(97)	6
st_4 [mg^{-1}]	Stimulation factor of GLP-1 production by late signal	$26.2 \cdot 10^{-5}$	3	–	–
SD_{glp} [pmol l^{-1}]	Additive error	0.998	5	–	–
CV_{glp} (%) [pmol l^{-1}]	Proportional error	9	–	–	–

The f is obtained from Ref. [18] and k_a is estimated from glucose/insulin data

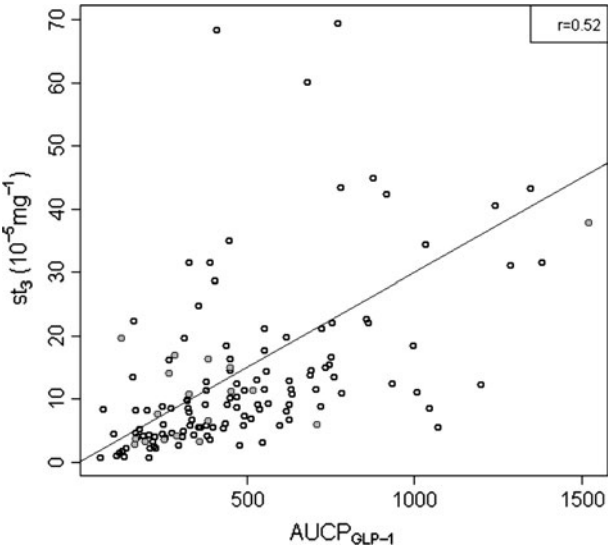


Fig. 6 Individual predictions of parameter st_3 versus $AUCP_{GLP\text{-}1}$ calculated as AUC from 0–60 min. above baseline values. *Open circles*: NGTs, *Gray filled circles*: IFG-IGT-T2Ds. *Line* presents relation: $st_3 = 0.03\ AUCP_{GLP\text{-}1}$, obtained using perpendicular least squares

elimination pathway. The model for glucose/insulin was estimated separately from the GLP-1 secretion model. This was done in order not to bias the estimation of glucose absorption towards the prediction of GLP-1 concentrations. Besides, the

Apotex v. Novo - IPR2024-00631
Petitioner Apotex Exhibit 1053-0010
MPI EXHIBIT 1053 PAGE 10

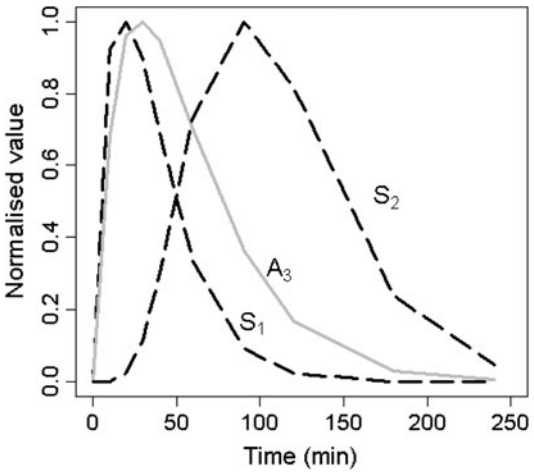


Fig. 7 Normalized mean of simulations of compartments S_1, A_3 and S_2 versus time

simultaneous estimation was very time-consuming causing separate estimation to be preferred.

The GLP-1 secretion model was successfully applied to a mixed-effects model setting using NONMEM VI, thus providing both information about intra-variability and inter-variability in the studied population.

To our knowledge compartmental modelling of GLP-1 secretion following an OGTT has not been performed previously. As observed from our individual profiles there is very high variability between subjects and the response is considered complex which relates to the fact that determinants of the secretion are not fully understood. Based on this we initially started out using a simple indirect response model using one stimulus related solely to the glucose absorption rate. This stimulus was not adequate to describe the GLP-1 secretion and we observed that two phases of secretion could be identified. Based on the estimation of the rate constants k_b and k_c, the peaks of these stimuli were observed to be around 25 and 100 min. This seems to be consistent with the GLP-1 profiles following a mixed meal [21] indicating maximum GLP-1 concentrations shortly after the peak stimulation times.

The fast response (peak around 25 min.) is hypothesized to be caused mainly by nutrients in the duodenum activating a proximal—distal neuroendocrine loop stimulating GLP-1 secretion from L-cells and colon (3). In our study we estimated the rate constant (k_c) related to the first-phase to be significantly faster than the rate constant (k_a) related to glucose absorption. This provides evidence for the possibility of the neuroendocrine regulation of L-cell secretion (3), although more insights could be gained from further experiments.

In this study we chose not to perform covariate analysis on the individual parameters for secretion, and did thus also not analyse the effect of disease state on the obtained estimates. Such an analysis belongs to another study, and must be performed with data that has more subjects identified with T2D.

The developed model should be seen as a tool that in future can be applied to investigate factors such as disease state, drug effect, or ethnicity on the parameters characterizing GLP-1 secretion.

Apotex v. Novo - IPR2024-00631
Petitioner Apotex Exhibit 1053-0011

MPI EXHIBIT 1053 PAGE 11

Estimating the rate of absorption of glucose without the use of tracer has been a subject in various publications [18, 22]. We applied a simple approach using only one parameter without information from tracer kinetics.

In order to investigate the dependence of our approach on different glucose absorption models, we implemented two alternative models [18, 22]. The objective function values, population fittings and correlation obtained between st_3 and $AUCP_{GLP\text{-}1}$ appeared similar to the present results. A clear drawback of our study is that the absorption rate for glucose is not necessarily captured with high accuracy. It will be of future interest to see how the model performs knowing the rate of absorption obtained with a tracer [22, 23].

Another limitation of this study is that only one dose level of the OGTT was administered. Possible non-linearities in the GLP-1 response are thus unidentifiable. For further model development it would be informative to repeat the experiments performed in this analysis with different glucose doses.

Regarding the number of transit compartments one could argue that the possibility of having different individual numbers would be reasonable. This was tested using an explicit solution [17], but was found to cause the model not to be uniquely identifiable thus causing unstable estimation of parameters. Instead we chose to have IIV on k_b, thus enabling individual differences in time of onset of S_2. In spite of the fact that IIV was only 12% in k_b values, we observed significantly higher OFV and a worse model fit. That was the reason for having k_b not fixed to 0.

The value of k_{out_GLP1} indicates a half-life of total GLP-1 of around 10 min. This agrees with values in the range of 3–11 min obtained experimentally in vivo [13], although it seems to be slightly higher than values obtained for active GLP-1 (7–36), specifically measured in humans [4, 24, 25]. As Holst et al. [16] describe, there are different types of GLP-1 and in this study the measured concentration reflects the sum of the active GLP-1 (7–36) and the inactive form, GLP-1 (9–37). The inactive form has a much longer half-life [16] which will be the main determinant for the half-life. In general it is important to note that the degradation of GLP-1 (7–36) is known to be fairly complex and involves both an inactivation in the gut and degradation in liver which is not taken into account here. It would thus be of future interest to build a more complex model based on data obtained in different tissues and from the different metabolites.

Acknowledgments This study was partly supported by NIH Grant GM 57980 for WJJ and WG.

References

1. Vilsboll T, Agerso H, Krarup T, Holst JJ (2003) Similar elimination rates of glucagon-like peptide-1 in obese type 2 diabetic patients and healthy subjects. J Clin Endocrinol Metab 88(1):220–224
2. Brandt A, Katschinski M, Arnold R, Polonsky KS, Goke B, Byrne MM (2001) GLP-1-induced alterations in the glucose-stimulated insulin secretory dose-response curve. Am J Physiol Endocrinol Metab 281(2):E242–E247
3. Lim GE, Brubaker PL (2006) Glucagon-like peptide 1 secretion by the L-cell. Diabetes 55(Suppl 2): S70–S77
4. Meier JJ, Nauck MA, Kranz D, Holst JJ, Deacon CF, Gaeckler D, Schmidt WE, Gallwitz B (2004) Secretion, degradation, and elimination of glucagon-like peptide 1 and gastric inhibitory polypeptide in patients with chronic renal insufficiency and healthy control subjects. Diabetes 53(3):654–662

Apotex v. Novo - IPR2024-00631
Petitioner Apotex Exhibit 1053-0012
MPI EXHIBIT 1053 PAGE 12

5. Rask E, Olsson T, Söderberg S, Holst JJ, Tura A, Pacini G, Ahrén B (2004) Insulin secretion and incretin hormones after oral glucose in non-obese subjects with impaired glucose tolerance. Metabolism 53(5):624–631
6. Knop FK, Vilsbøll T, Højberg PV, Larsen S, Madsbad S, Vølund A, Holst JJ, Krarup T (2007) Reduced incretin effect in type 2 diabetes. Diabetes 56(8):1951–1959
7. Dayneka NL, Garg V, Jusko WJ (1993) Comparison of four basic models of indirect pharmacodynamic responses. J Pharmacokinet Pharmacodyn 21(4):457–478
8. Toft-Nielsen MB, Damholt MB, Madsbad S, Hilsted LM, Hughes TE, Michelsen BK, Holst JJ (2001) Determinants of the impaired secretion of glucagon-like peptide-1 in type 2 diabetic patients. J Clin Endocrinol Metab 86(8):3717–3723
9. Hansen T, Drivsholm T, Urhammer SA, Palacios RT, Vølund A, Borch-Johnsen K, Pedersen O (2007) The BIGTT test. Diabetes Care 30(2):257–262
10. American Diabetes Association (2004) Diagnosis and classification of diabetes mellitus. Diabetes Care 30(suppl 1):S5–S10
11. Andersen L, Dinesen B, Jorgensen P, Poulsen F, Roder M (1993) Enzyme immunoassay for intact human insulin in serum or plasma. Clin Chem 39(4):578–582
12. Orskov C, Rabenhøj L, Wettergren A, Kofod H, Holst JJ (1994) Tissue and plasma concentrations of amidated and glycine-extended glucagon-like peptide I in humans. Diabetes 43(4):535–539
13. Deacon CF, Pridal L, Klarskov L, Olesen M, Holst JJ (1996) Glucagon-like peptide 1 undergoes differential tissue-specific metabolism in the anesthetized pig. Am J Physiol Endocrinol Metab 271(3):E458–E464
14. Lima JJ, Matsushima N, Kissoon N, Wang J, Sylvester JE, Jusko WJ (2004) Modeling the metabolic effects of terbutaline in [beta]2-adrenergic receptor diplotypes[ast]. Clin Pharmacol Ther 76(1): 27–37
15. Woo S, Pawaskar D, Jusko W (2009) Methods of utilizing baseline values for indirect response models. J Pharmacokinet Pharmacodyn 36(5):381–405
16. Holst JJ (2007) The physiology of glucagon-like peptide 1. Physiol Rev 87(4):1409–1439
17. Savic R, Jonker D, Kerbusch T, Karlsson M (2007) Implementation of a transit compartment model for describing drug absorption in pharmacokinetic studies. J Pharmacokinet Pharmacodyn 34(5):711–726
18. Silber HE, Frey N, Karlsson MO (2010) An integrated glucose-insulin model to describe oral glucose tolerance test data in healthy volunteers. J Clin Pharmacol 50(3):246–256
19. Møller J, Overgaard R, Madsen H, Hansen T, Pedersen O, Ingwersen S (2010) Predictive performance for population models using stochastic differential equations applied on data from an oral glucose tolerance test. J Pharmacokinet Pharmacodyn 37(1):85–98
20. Savic R, Karlsson M (2009) Importance of shrinkage in empirical Bayes estimates for diagnostics: problems and solutions. AAPS J 11(3):558–569
21. Rask E, Olsson T, Søderberg S, Johnson O, Seckl J, Holst JJ, Ahrén B (2001) Impaired incretin response after a mixed meal is associated with insulin resistance in nondiabetic men. Diabetes Care 24(9):1640–1645
22. Dalla Man C, Caumo A, Basu R, Rizza R, Toffolo G, Cobelli C (2004) Minimal model estimation of glucose absorption and insulin sensitivity from oral test: validation with a tracer method. Am J Physiol Endocrinol Metab 287(4):E637–E643
23. Thomaseth K, Pavan A, Berria R, Glass L, DeFronzo R, Gastaldelli A (2008) Model-based assessment of insulin sensitivity of glucose disposal and endogenous glucose production from double-tracer oral glucose tolerance test. Comput Methods Prog Biomed 89(2):132–140
24. Orskov C, Wettergren A, Holst JJ (1993) Biological effects and metabolic rates of glucagonlike peptide-1 7–36 amide and glucagonlike peptide-1 7–37 in healthy subjects are indistinguishable. Diabetes 42(5):658–661
25. Kreymann B, Ghatei MA, Williams G, Bloom SR (1987) Glucagon-like peptide-1 7–36: a physiological incretin in man. Lancet 330(8571):1300–1304

Apotex v. Novo - IPR2024-00631
Petitioner Apotex Exhibit 1053-0013

MPI EXHIBIT 1053 PAGE 13